

## The Magnetic and Magnetostrictive Properties of Melt-Spun Ribbons of B Containing Terfenol-D Alloys

S. R. Kim, S. Y. Kang\* and S. H. Lim

Magnetic Materials Lab., Korea Institute of Science and Technology, P.O. Box 131,  
Cheongryang, Seoul, 130-650, Korea

\*Dept. of Metallurgical Engr., Korea University, Seoul, 136-701

(Received 26 March 1997)

The magnetic and magnetostrictive properties of melt-spun ribbons of the alloys  $(R_{0.33}Fe_{0.67})_{1-x}B_x$  ( $R=Tb_{0.3}Dy_{0.7}$  and  $0 \leq x \leq 0.06$ ) are investigated as a function of wheel speed during melt-quenching. The saturation magnetization of the alloys with a crystalline phase ranges from 70 to 80 emu/g and does not vary substantially with the B content. The saturation magnetization of an amorphous phase, which is formed at the condition of high wheel speed and high B content, is reduced significantly, however. The coercive force is minimum at  $x=0.02$  and increases monotonously with the further increase of B content when the microstructure mainly consists of a crystalline phase, but again it is reduced significantly by the formation of an amorphous phase. The low field sensitivity of magnetostriction with magnetic field is found to be good for the alloys with  $x \leq 0.04$  over a wide range of wheel speed. This magnetostrictive behavior is in contrast with that observed previously for Dy-Fe and Tb-Fe based alloys and is thought to be due to low intrinsic magnetocrystalline anisotropy of the compound.

### 1. Introduction

Cubic Laves phase  $TbFe_2$  compound is known to exhibit the largest magnetostriction of about 2000 ppm at room temperature [1]. However, since the magnetocrystalline anisotropy of the compound is also very large, a large magnetic field is required to obtain a large strain which may cause a serious problem in the practical applications of the compound. Many efforts were made to solve the problem through a suitable alloy design in the early days of research on the compound; one notable outcome is the development of  $Tb_{0.3}Dy_{0.7}Fe_2$  commercially known as Terfenol-D [2]. Since late eighties, the reduction in the magnetocrystalline anisotropy has been attempted by suitably controlling the microstructure, more specifically, by refining the grain size [3-6]. The theoretical background for this is that the magnetocrystalline anisotropy is "effectively" reduced when the size of grains ( $D$ ) is smaller than the ferromagnetic exchange length ( $L_{ex}$ ) [7]. By using the random walk method in the random anisotropy model, the effective magnetocrystalline anisotropy ( $K_{eff}$ ) is related to the (intrinsic) anisotropy ( $K$ ) by the equation [8];  $K_{eff} = K / \sqrt{N}$  where  $N$  is the number of grains within the ferromagnetic

coupling region.

The grain size refinement has mainly been done by firstly producing an amorphous phase using a rapid-quenching method and then subsequently annealing the amorphous phase. At a suitable annealing condition, ultrafine grains with the size of about 10 nm were formed and a large improvement in the magnetic softness was observed as a result of reduction in the anisotropy [3]. More recently, however, it was shown by the present authors for Dy-Fe and Tb-Fe based alloys that homogeneous and ultrafine grains were obtained even in the as-spun state [5,6]. This was made possible at a suitable quenching rate, together with the addition of a suitable amount of B to the alloys. The ribbons having the nanocrystalline grain structure were found to exhibit a very good magnetic softness indicated by a large increase in the magnetostrain at low magnetic fields. The element B was found to play an important role in the microstructural modification.

In this work, a similar approach is made for the Tb-Dy-Fe based alloys in order to see how the magnetic and magnetostrictive properties vary with the quenching rate during a rapid solidification process and the content of B in the alloy. The alloy system investigated is  $(R_{0.33}Fe_{0.67})_{1-x}B_x$

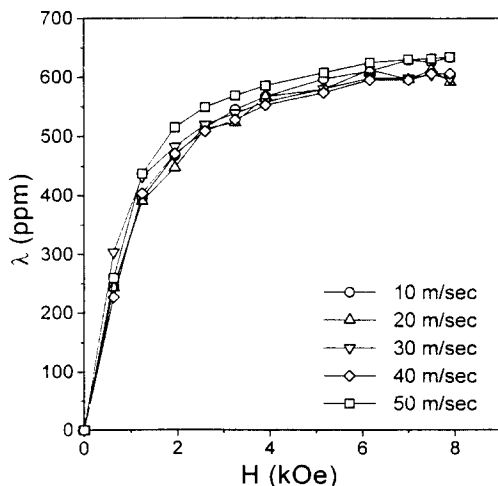
with  $R=Tb_{0.3}Dy_{0.7}$  and  $x=0, 0.02, 0.04$  and  $0.06$ .

### 2. Experimental Details

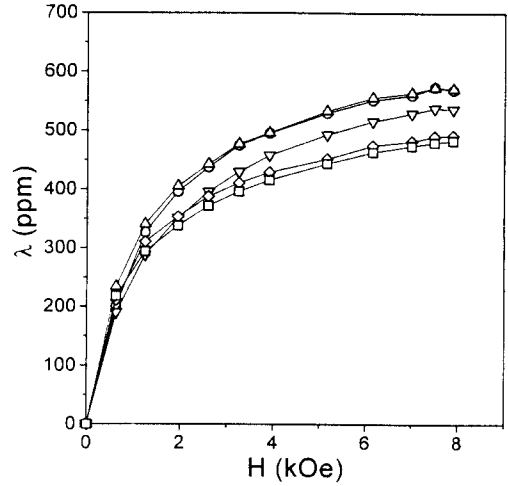
The alloys were induction-melted in an inert atmosphere. Subsequent melt-spinning was carried out also in an inert atmosphere. In the present experiments, all the fabrication parameters were fixed except for the wheel speed which was varied over a wide range from 10 to 50 m/sec. The melt temperature was maintained at just above the melting point. The orifice diameter was about 0.5 mm and the chamber and ejecting Ar pressures were  $2.1 \times 10^{-2}$  and  $1.85 \times 10^{-1}$  MPa, respectively. The magnetostriction ( $\lambda$ ) was measured by a three-terminal capacitance method [9] at magnetic fields ( $H$ ) up to 8 kOe. The magnetostriction transducer consists of a moving electrode and a fixed one, a ribbon with a length of about 10 mm connecting the two electrodes. The change in the distance between the two electrodes (and hence the capacitance change of the transducer) results from the linear magnetostriction which can be obtained by using the eq. (4) of ref. [9]. The value of  $\lambda$  presented in this paper is so called the saturation magnetostriction at a given field and is obtained by the relation  $\lambda = \frac{2}{3} (\lambda_{\parallel} - \lambda_{\perp})$ . Here  $\lambda_{\parallel}$  and  $\lambda_{\perp}$  are respectively the values of magnetostriction measured in the parallel and the transverse directions in the ribbon plane and the difference ( $\lambda_{\parallel} - \lambda_{\perp}$ ) corresponds to the peak to peak value when rotating in-plane magnetic fields are applied. The microstructure was mainly examined by X-ray diffraction with Cu  $K\alpha$  radiation and, in some cases, also by transmission electron microscopy (TEM). The magnetic properties were measured by using a vibrating sample magnetometer with a maximum magnetic field of 15 kOe.

### 3. Results and Discussion

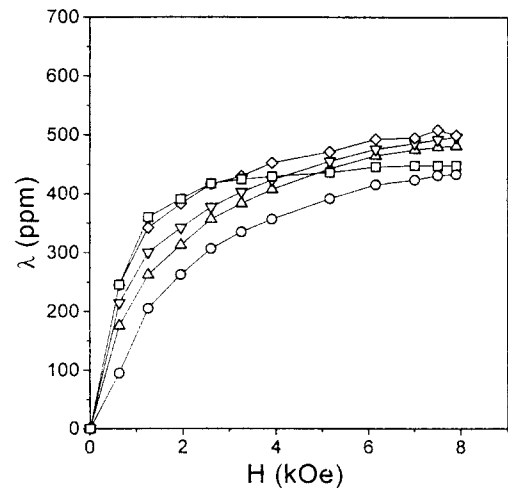
The results for  $\lambda$ - $H$  curves at various quenching speeds are shown in Figs.1(a)-(d) for the alloys  $x=0, 0.02, 0.04$  and



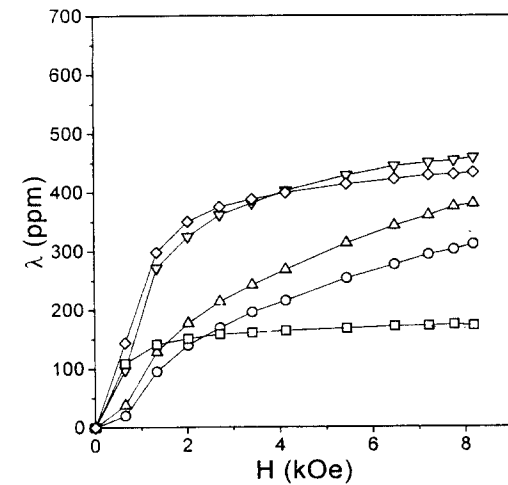
(a)



(b)



(c)



(d)

Fig.1 The  $\lambda$  - $H$  plots for the alloys  $(R_{0.33}Fe_{0.67})_{1-x}B_x$  with  $R=Tb_{0.3}Dy_{0.7}$ : (a)  $x=0$ , (b)  $x=0.02$ , (c)  $x=0.04$  and (d)  $x=0.06$ .

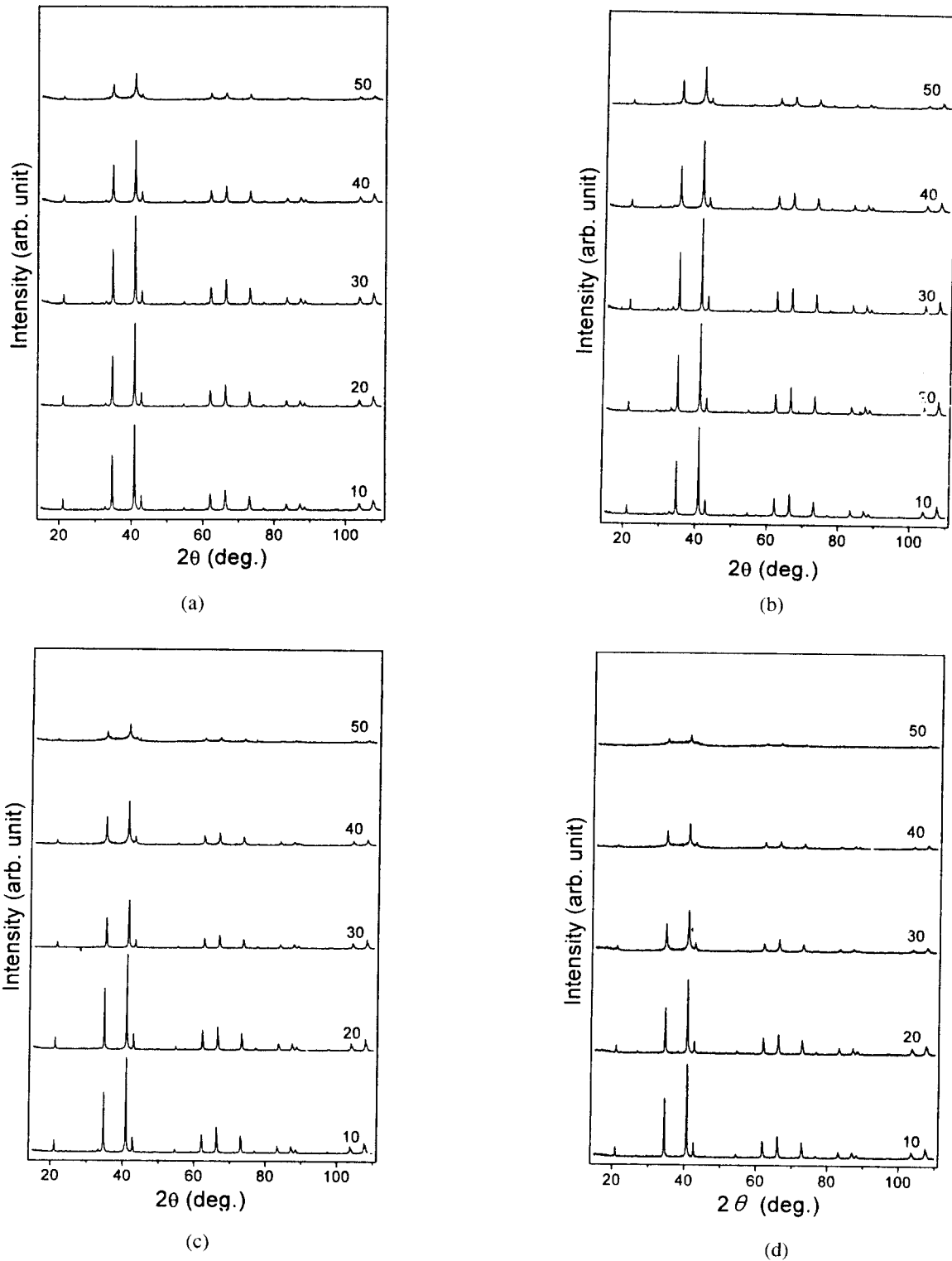


Fig.2 The X-ray diffraction patterns for the alloys  $(R_{0.33}Fe_{0.67})_{1-x}B_x$  with  $R=Tb_{0.3}Dy_{0.7}$ ; (a)  $x=0$ , (b)  $x=0.02$ , (c)  $x=0.04$  and (d)  $x=0.06$ . The numbers on the diffraction patterns denote the wheel speed in m/sec

0.06, respectively. X-ray diffraction patterns for the respective alloys are also displayed in Figs.2(a)-(d).

It is seen from Fig.1(a) for the B-free alloy that, even at low magnetic fields, the value of  $\lambda$  increases sensitively with increasing magnetic field for all the wheel speeds

investigated in this work and the  $\lambda$ - $H$  behavior is nearly independent of the wheel speed. This is in striking contrast with the behavior previously observed in Dy-Fe [5] and Tb-Fe based alloys [6], where the sensitivity of  $\lambda$  with  $H$  depends on the wheel speed and it generally improves with

increasing wheel speed until optimum wheel speed is reached. These magnetostrictive characteristics, however, are expected, since the value of  $K$  of the alloy is very small (if not zero) and hence the reduction of  $K$  by grain refinement is thought to be minimal. Sharp crystalline peaks of the cubic Laves (Tb, Dy)Fe<sub>2</sub> phase are seen in the diffraction patterns at the wheel speeds of 10-30 m/sec and the intensity of the peaks remains nearly unchanged in this range of wheel speed. However, the peak intensity is decreased at 40 m/sec and, at the highest wheel speed of 50 m/sec, the peak intensity becomes weak and the broadening of the peaks occurs, indicative of grain refinement. The grain size at 50 m/sec determined from the Scherrer equation is about 20 nm.

With the addition of B to the alloy, the  $\lambda$ - $H$  curves differ from the B-free alloy depending on the wheel speed and the difference in the  $\lambda$ - $H$  behavior with the wheel speed tends to increase with the amount of B. In the case of the  $x=0.02$  alloy, the shape of  $\lambda$ - $H$  curves is similar for all the wheel speeds and is also similar to that shown in Fig.1(a) for the B-free alloy, but the magnitude of  $\lambda$  at a given magnetic field decreases monotonously with increasing wheel speed.

The wheel speed dependence of the  $\lambda$ - $H$  behavior differs substantially for the  $x=0.04$  alloy. Two main differences may be noted. Firstly, the shape of  $\lambda$ - $H$  curves of the ribbons fabricated at the wheel speed of 40 m/sec and below is similar to that shown in Figs.1(a) and (b) for the alloys with  $x \leq 0.02$ , but that of the ribbon quenched at 50 m/sec differs substantially, the saturation being reached at a low magnetic field. Secondly, the magnitude of  $\lambda$  at a given magnetic field now increases monotonously as the wheel speed increases from 10 to 40 m/sec, this behavior being completely opposite to that for the  $x=0.02$  alloy.

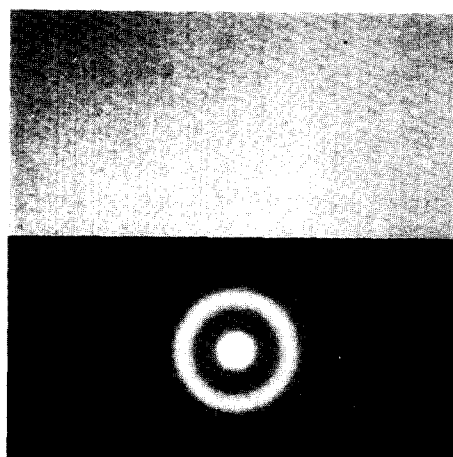
These results may be explained in terms of the formation of an amorphous phase and the increase of  $K$  with increasing B content. The saturation magnetostriction, in most cases, is reduced by the formation of an amorphous phase. The reduction of  $K$  of the Tb-Dy-Fe alloy is known to be made by a cancellation of the anisotropy constants of Dy and Tb with opposite signs and this is possible in the crystal symmetry of the cubic Laves (Tb,Dy)Fe<sub>2</sub> phase [1]. In the case of an alloy with a Tb/Dy ratio where a complete cancellation of the anisotropy occurs, the cancellation may not be achieved completely if the cubic structure is distorted, for example and as in the present case, by the addition of B. It is thought that the element B with its small atomic radius compared to the other elements resides in interstitial sites of the (Tb,Dy)Fe<sub>2</sub> cubic structure. With this consideration, it is likely that the magnitude of  $K$  is not negligibly small for the B containing alloys and it increases with the amount of B in the alloy.

The monotonic decrease of  $\lambda$  with the wheel speed for the  $x=0.02$  alloy is originally thought to be due to the formation of an amorphous phase, since the amount of an amorphous

phase is likely to increase with increasing wheel speed. The formation of an amorphous phase, however, is not clearly identified by the diffraction patterns shown in Fig.2(b) with the exception for the ribbons fabricated at 50 m/sec. More work is necessary to clarify the wheel speed dependence of the  $\lambda$ - $H$  behavior.



(a)



(b)

Fig.3 Transmission electron micrographs (both the bright and dark field images) and selected area diffraction patterns for the ribbons of the alloys  $(R_{0.33}Fe_{0.67})_{1-x}B_x$  with  $R=Tb_{0.3}Dy_{0.7}$  fabricated at 50 m/sec; (a)  $x=0.04$  and (b)  $x=0.06$ .

The  $\lambda$ - $H$  behavior for the  $x=0.04$  alloy is identical to that for Tb-Fe and Dy-Fe based alloys with large values of  $K$  [5,6]. This may indicate that the magnitude of  $K$  of the  $x=0.04$  alloy is not small and the effective anisotropy is reduced by grain refinement and/or amorphization. The shape of  $\lambda$ - $H$  curve at 50 m/sec with low saturation magnetic field is typical to that of an amorphous phase. From the X-ray results (Fig.2(c)), the microstructure at 50 m/sec is thought to consist of a mixture of an amorphous phase and a very fine crystalline phase, which is confirmed by TEM as shown in Fig.3(a).

The explanation of the  $\lambda$ - $H$  results for the  $x=0.04$  alloy by the formation of an amorphous phase and the increase of  $K$  with the increase of B content is further verified by the results for the  $x=0.06$  alloy shown in Fig.2(d). The sensitivity of  $\lambda$  with  $H$  is very poor at low wheel speeds of 10 and 20 m/sec, indicating that the value of  $K$  is further increased but it is not effectively reduced in this wheel speed range. The sensitivity of  $\lambda$  with  $H$  at low fields, however, increases with the increase of the wheel speed. The shape of  $\lambda$ - $H$  curve of the ribbon at 50 m/sec is typical to that of an amorphous phase. It is seen from Fig.2(d) that the microstructure at this wheel speed mainly consists of an amorphous phase with a trace of the crystalline phase, although no crystalline precipitates were observed by TEM (Fig.3(b)). The saturation magnetostriction of the ribbon with an amorphous structure is substantially smaller than that of crystalline structure, indicating that the saturation magnetostriction is reduced by the formation of an amorphous phase. It is noted from Figs.1(a)-(d) that the value of  $\lambda$  tends to decrease with increasing B content, which is in agreement with the results observed for Tb-Fe and Dy-Fe based alloys [5,6].

Let us now consider the magnetic properties. The results for the saturation magnetization and the coercive force are shown respectively in Figs. 4 and 5 as a function of wheel speed. In these figures, the results of the TbFe<sub>2</sub> based alloy with 2 at.% B are also shown for comparison. The magnetization at 15 kOe ( $M_{15}$ ) is taken as the saturation magnetization and, since most of the present alloys saturate at a magnetic field well below 15 kOe, the magnitude of  $M_{15}$  is practically identical to the saturation magnetization. The coercive force ( $H_c$ ) is obtained by applying the maximum magnetic field of 15 kOe.

The magnitude of saturation magnetization does not vary substantially with the wheel speed for the alloys with  $x \leq 0.04$  and, for these alloys, the value ranges from 70 to 80 emu/g. In the case of the alloy with the highest B content, however, a significant reduction is observed at the high wheel speeds of 40 and 50 m/sec. This is clearly related to the formation of an amorphous phase, since the saturation magnetization as well as the saturation magnetostriction is generally reduced by the formation of an amorphous phase

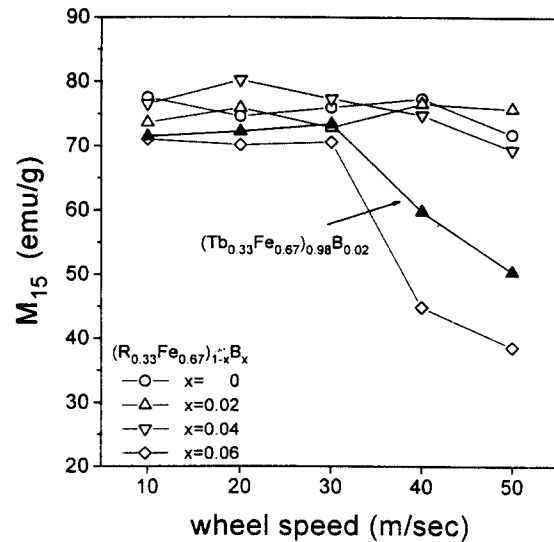


Fig.4 The saturation magnetization as a function of wheel speed for the alloys  $(R_{0.33}Fe_{0.67})_{1-x}B_x$  with  $R=Tb_{0.3}Dy_{0.7}$  and  $x=0, 0.02, 0.04$  and  $0.06$ . The results for the Dy-free TbFe<sub>2</sub> alloy with 2 at.% B are also shown for comparison.

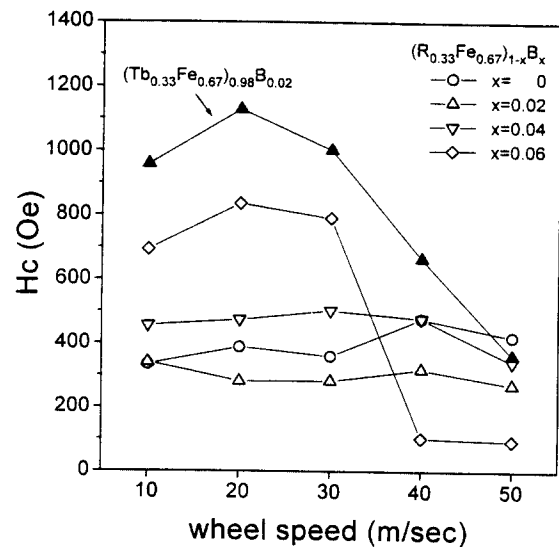


Fig.5 The coercive force as a function of wheel speed for the alloys  $(R_{0.33}Fe_{0.67})_{1-x}B_x$  with  $R=Tb_{0.3}Dy_{0.7}$  and  $x=0, 0.02, 0.04$  and  $0.06$ . The results for the Dy-free TbFe<sub>2</sub> alloy with 2 at.% B are also shown for comparison.

[10]. The wheel speed dependence of saturation magnetization of the TbFe<sub>2</sub> alloy with 2 at.% B is similar to that of the  $x=0.06$  alloy, although the reduction in  $M_{15}$  is smaller in the TbFe<sub>2</sub> based alloy. Again, the reduction of saturation magnetization of the B containing TbFe<sub>2</sub> alloy is due to the formation of an amorphous phase, which is confirmed by X-ray diffracton and TEM [6,11]. The present results may indicate that the glass forming ability of TbFe<sub>2</sub> alloy is reduced by the partial substitution of Dy for Tb, since Tb-Dy-Fe based alloys with a similar or even larger

amount of B does not form an amorphous phase in the wheel speed range investigated in the present work. This reduced glass forming ability of the present Tb-Dy-Fe-B alloys is actually observed from the microstructural examination, for example the X-ray diffraction results, where the intensity and the width of diffraction peaks vary less sensitively with the wheel speed than the other alloy systems including the Tb-Fe based alloys [6,11].

A very large difference is seen in the coercive force with the B content, the magnitude ranging from 95 to 835 Oe. The wheel speed dependence of the coercive force, however, is similar to that of the saturation magnetization in the sense that the magnitude of the coercive force does not vary substantially with the wheel speed except for the condition of high wheel speed and high B content where an amorphous phase is formed. For the ribbons composed of mainly crystalline phase, the coercive force decreases as the B content increases from 0 to 2 at.% but, with the further increase of the B content, the coercive force increases with increasing B content. These results for the coercive force further support the fact that the value of  $K$  increases with increasing B content. The very large reduction of the coercive force for the ribbons of the  $x=0.06$  alloy fabricated at the wheel speed of 40 or 50 m/sec is obviously due to the reduction of the effective magnetocrystalline anisotropy by the formation of an amorphous phase. The coercive force of the B containing TbFe<sub>2</sub> alloy is large compared to Tb-Dy-Fe based alloys and this is thought to be a large  $K$  value, among other things. The continuous decrease of the coercive force of the TbFe<sub>2</sub> based alloy with the increase of wheel speed from 20 to 50 m/sec is well expected and this results from the decrease of the effective anisotropy by the grain refinement and/or amorphization.

#### 4. Conclusions

From a systematic investigation on the magnetostriction of melt-spun ribbons of the alloys  $(R_{0.33}Fe_{0.67})_{1-x}B_x$  ( $R=Tb_{0.3}Dy_{0.7}$  and  $0 \leq x \leq 0.06$ ), it has been found that good low field sensitivity of  $\lambda$  with  $H$  is achieved over a wide range of wheel speed for the alloys with  $x \leq 0.04$  and the sensitivity improves with decreasing B content. The  $\lambda$ - $H$  behavior is

nearly independent of the wheel speed for the B-free alloy, but it depends on the wheel speed for the alloys with B, the wheel speed dependence of  $\lambda$ - $H$  behavior increasing with the B content. The saturation magnetization of the alloys with crystalline phase does not vary substantially with the B content but that of an amorphous phase, which is formed at the condition of high wheel speed and high B content, is reduced significantly. The coercive force is minimum at the B content of 2 at.% ( $x=0.02$ ) and increases monotonously with the further increase of B content when the microstructure mainly consists of a crystalline phase, but again it is reduced significantly by the formation of an amorphous phase. The present magnetic and magnetostrictive results have mainly been explained in terms of the formation of an amorphous phase and the increase of intrinsic magnetocrystalline anisotropy with the addition of B.

#### References

- [1] A. E. Clark, Ferromagnetic Materials, vol.1, E. P. Wohlfarth (Ed.), North-Holland, Amsterdam(1980) chap.7
- [2] A. E. Clark, AIP Conf. Proc. No.18, New York: American Institute of Physics, New York(1974) p.1015
- [3] S. Kikuchi, T. Tanaka, S. Sugimoto, M. Okada, M. Homma and K. Arai, J. Magn. Soc. Jpn., **17**, 267(1993)
- [4] T. Oike, S. Ishio and T. Miyazaki, J. Magn. Soc. Jpn., **17**, 271 (1993)
- [5] S. H. Lim, T. H. Noh, I. K. Kang, S. R. Kim and S. R. Lee, J. Appl. Phys., **76**(10), 7021(1994)
- [6] S. H. Lim, S. R. Kim and H. J. Kim, IEEE Trans. Magn., **32**(5), 4770(1996)
- [7] G. Herzer, IEEE Trans. Magn., **26**, 1397(1990)
- [8] A. Hernando and M. Vazquez, Rapidly Solidified Alloys, vol.1 H. H. Liebermann(Ed.), New York: Marcel Dekker(1993) chap.17
- [9] Y. H. Lee, Y. D. Shin, K. H. Lee, M. Y. Kim and J. R. Rhee, IEEE Trans. Magn., **31**(6), 3397(1995)
- [10] P. Hansen, Handbook of Magnetic Materials, vol.6, K. H. Buschow (Ed.), North-Holland, Amsterdam(1991) chap.4
- [11] S. R. Kim, S. Y. Kang and S. H. Lim, (to be published)